2014

INVESTIGATION OF CARDIAC ELECTROPHYSIOLOGY IN HUMAN VENTRICULAR TISSUE

Kathleen Brownson
University of Kentucky, katebrownson@gmail.com

STUDENT AGREEMENT:

I represent that my thesis or dissertation and abstract are my original work. Proper attribution has been given to all outside sources. I understand that I am solely responsible for obtaining any needed copyright permissions. I have obtained needed written permission statement(s) from the owner(s) of each third-party copyrighted matter to be included in my work, allowing electronic distribution (if such use is not permitted by the fair use doctrine) which will be submitted to UKnowledge as Additional File.

I hereby grant to The University of Kentucky and its agents the irrevocable, non-exclusive, and royalty-free license to archive and make accessible my work in whole or in part in all forms of media, now or hereafter known. I agree that the document mentioned above may be made available immediately for worldwide access unless an embargo applies.

I retain all other ownership rights to the copyright of my work. I also retain the right to use in future works (such as articles or books) all or part of my work. I understand that I am free to register the copyright to my work.

REVIEW, APPROVAL AND ACCEPTANCE

The document mentioned above has been reviewed and accepted by the student's advisor, on behalf of the advisory committee, and by the Director of Graduate Studies (DGS), on behalf of the program; we verify that this is the final, approved version of the student's thesis including all changes required by the advisory committee. The undersigned agree to abide by the statements above.

Kathleen Brownson, Student

Dr. Abhijit Patwardhan, Major Professor

Dr. Abhijit Patwardhan, Director of Graduate Studies

INVESTIGATION OF CARDIAC ELECTROPHYSIOLOGY IN HUMAN VENTRICULAR TISSUE

THESIS

A thesis submitted in partial fulfillment of the
requirements for the degree of Master of Science in
Biomedical Engineering in the College of Engineering
at the University of Kentucky

By

Kathleen Brownson

Lexington, Kentucky

Director: Dr. Abhijit Patwardhan, Professor of Biomedical Engineering

Lexington, Kentucky

2014

ABSTRACT OF THESIS

INVESTIGATION OF CARDIAC ELECTROPHYSIOLOGY IN HUMAN VENTRICULAR TISSUE

Individuals with cardiomyopathy are at higher risk to die from sudden cardiac arrest than those with non-failing (NF) hearts. This study examined the differences in electrical properties of failing and NF human hearts in terms of cardiac memory through explicit control of diastolic intervals in a sinusoidal fashion, restitution of action potential duration (APD) through standard and dynamic pacing protocols, maximum rate of depolarization and APD alternans. Recordings of transmembrane potentials were made in tissues extracted from patients with heart failure and one donor NF heart. Computational simulations were performed using the O'Hara Rudy model for generating surrogates of control data. Significant differences were seen between left ventricular (LV) tissue and NF LV tissue in tilt, and measures of memory in terms of area and thickness during the sinusoidal 400ms protocol. Minimum delay was also significantly higher in the failing LV during the sinusoidal 150ms protocol. Failing tissues showed a higher restitution slope and prolonged AP which is consistent with previous studies and is hypothesized to contribute to the increased susceptibility to unstable alternans. This study further explored how disease alters the electrical functioning of the heart and why these patients are at a higher risk of ventricular arrhythmia.

KEYWORDS: Restitution, Ventricle, Cardiac Memory, Action Potential Duration, Heart Failure

Kathleen Brownson

May 5, 2014

INVESTIGATION OF CARDIAC ELECTROPHYSIOLOGY IN HUMAN VENTRICULAR TISSUE

By

Kathleen Brownson

Dr. Abhijit Patwardhan
Director of Thesis

Dr. Abhijit Patwardhan
Director of Graduate Studies

May 5, 2014
Date

This thesis is dedicated to my family and friends for their never-ending love and support, especially Ryan. I could not have done this without you.

ACKNOWLEDGEMENTS

I would like to thank my advisor, Dr. Abhijit Patwardhan for his extensive knowledge and patience. I would also like to acknowledge Anuj Agarwal for his mentorship and Yihua Zhao for assistance with experiments.

TABLE OF CONTENTS

LIST OF TABLES

LIST OF FIGURES

Chapter 1 INTRODUCTION

More than 350,000 Americans die from cardiac arrest, i.e. sudden cardiac death (SCD) each year.[1] The majority of SCDs are caused by abnormal electrical activity in the heart, specifically the degeneration of ventricular tachycardia to ventricular fibrillation (v-fib). During v-fib, quivering of the ventricles prevents the normal contractions and relaxations needed to pump blood. Functioning of the heart is dependent on both electrical and mechanical factors. Those individuals with heart failure (HF), or previously mechanically weakened tissue, are more likely to suffer from ventricular arrhythmias and therefore SCD.[1, 2] Individuals with cardiomyopathy have substrates which differ from healthy hearts such as fibrosis, altered communication pathways and ion currents. These changed properties affect the electrical path, which may result in arrhythmia, not allowing uniform contractions from the ventricles. The study of cardiac electrophysiology of healthy and diseased hearts has led to a better understanding of mechanisms and prediction factors of lethal arrhythmia. This has been made possible by the organ-level study of electrocardiography (ECG) most commonly used in the clinical setting, and the cellular and tissue-level recordings of action potentials (APs) from myocytes. Cardiac restitution and memory are thought to play primary roles in dynamics of electrical activity in the heart. Restitution explains the relationship between action potential duration (APD) based on the previous diastolic interval (DI), while memory is exhibited by the dependence of APD on the previous APs. The characteristics of these properties have been studied with the hypothesis that a lower restitution slope and more memory allow for a more stable system that is not as likely to degenerate. Alternans of APD, which is beat-to-beat variability in properties of APs, has been heavily correlated with risk of arrhythmia.[3] In addition to the APD and repolarization characteristics, the rate of depolarization, dV/dt, is also a primary factor affecting conduction. In the present study, we characterized differences in memory, restitution, dV/dt and APD alternans between failing and non-failing (NF) ventricular tissues from patients undergoing left ventricular assist device (LVAD) placement or heart transplants at the University of Kentucky Hospital. Computational modeling was also used as a supplement to generate control data when examining differences in restitution.

Chapter 2 BACKGROUND

2.1 Electrical Activation of the Heart

Electrical activity begins at the sinoatrial node containing pacemaker cells. The conduction travels to the atrioventricular node which delays the activation, allowing the atria time to empty blood into the ventricles. The path then continues down the bundle of His, purkinje fibers, and apex before branching along the outer walls of the ventricles, expanding from endocardium to epicardium. The precise coordination between the electrochemical propagation of activity and mechanical movement is needed for normal cardiac functioning. These regular, coupled contractions from the ventricle are possible due to the functional syncytium created by gap junctions, which allows for the rapid flow of current between myocytes. Gap junctions are found in the intercalated discs between cells and are composed of a family of proteins, specifically connexin43 (Cx43). The change in voltage as each cell is activated can be measured through a transmembrane potential (TMP).

2.2 Transmembrane Potentials

The TMP is determined by the difference of intra- and extracellular ion concentrations. When a cell is stimulated, or electrically activated, an AP is produced by the flux of ions through transmembrane ion channels. Phases 0 through 4 of the cardiac ventricular AP are shown in Figure 2.1.

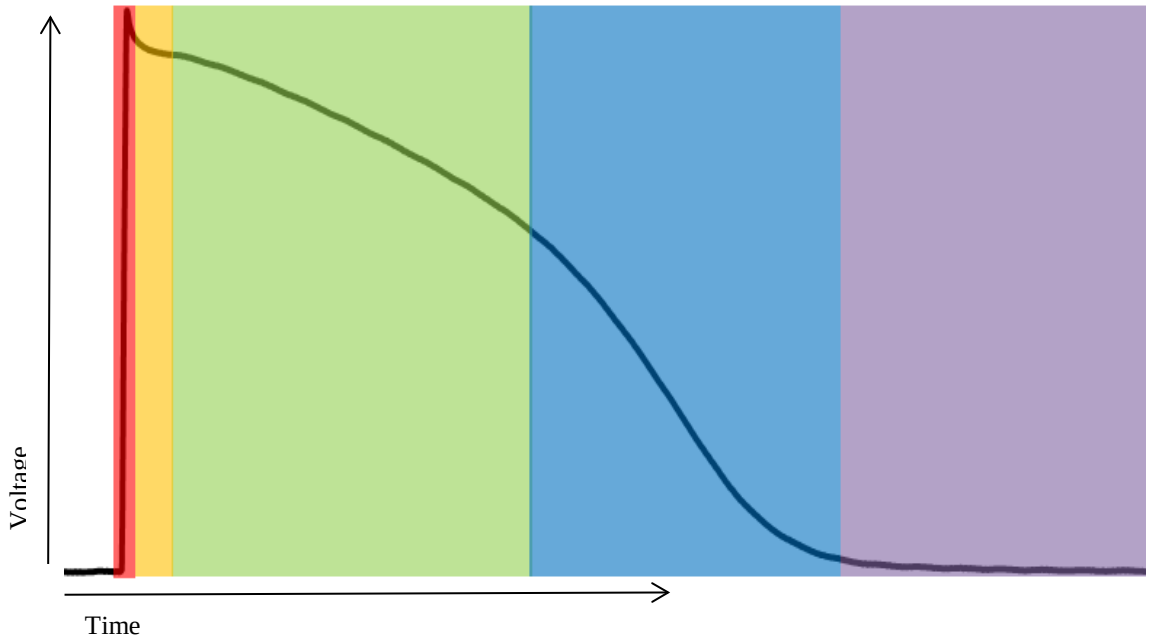

Figure 2.1 The phases of the ventricular cardiac action potential. Phases are shown from left to right with phase 0 (red), phase 1 (yellow), phase 2 (green), phase 3 (blue), and phase 4 (purple).

Phase 0: The cell is electrically stimulated and once the threshold potential has been met, an AP fires in an all-or-none manner. The quick depolarization results in the upstroke of the AP. The rate at which the depolarization occurs is computed using dV/dt. The maximum rate of depolarization is referred to by dV/dt_{max}. Depolarization is caused by the opening of Na^+ channels, which prompts Na^+ ions to rush into the cell.

Phase 1: After depolarization, there is a small dip in the AP when inactivation of the Na^+ channels occurs. Transient outward currents of K^+ and Cl^- occur and are known as Ito_1 and Ito_2, respectively. Ito_1 is known as the major contributor to the notch seen in the peak of the AP.

Phase 2: A plateau phase consists of inward Ca^{2+} (I_{Ca}) and outward K^+ through slow delayed rectifier K^+ channels (I_{Ks}). This phase aligns with the contraction of the muscle.

Phase 3: The cell then repolarizes when K^+ rushes out of the cell, and Ca^{2+} channels close. The net outward current then activates more K^+ channels to open including the inward rectifying I_{K1} and rapid delayed rectifier I_{Kr}.

Phase 4: The TMP then returns to a baseline known as the resting potential. The resting potential for ventricular myocytes is near -90mV. This potential is caused by the average of all ions' equilibrium potential and is most strongly controlled by K^+.

The combination of these and more minor currents is crucial in the continuation of the electrical activity across the tissue. The APD is defined as the duration from the beginning of depolarization to the end of the AP based on a determined percent repolarization, e.g. APD_{90} would be 90% repolarization. The time between APs is known as DI, the relaxation period which occurs during phase 4. Cycle length (CL) can be defined as the sum of APD and the preceding DI, or the time between activations of APs. The relationship between APD and DI has been widely used as a theoretical determinant of risk of arrhythmia.

2.3 Alternans of APD

APD alternans is changes in APD resulting in long-short-long durations for every other beat (See Figure 2.2). Alternans may be DI independent or DI dependent, i.e. existing with a constant DI or with alternating DI values, respectively.[4]

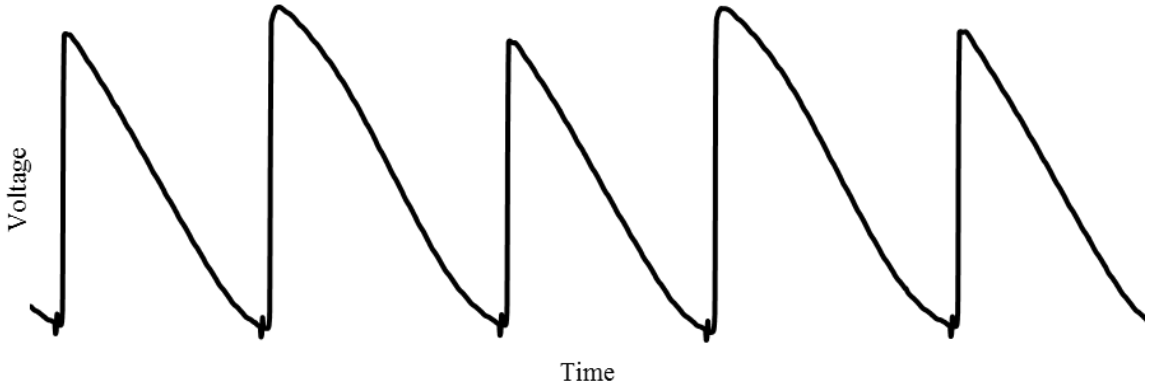

Figure 2.2 Example of APD alternans. APs with alternating APDs (as well as alternating AP amplitudes) from the human ventricle are shown. The notch prior to each AP is the stimulus artifact from artificial pacing. Note that the triangular shaped AP exists at faster pacing rates.

Unstable alternans may lead to block, where an AP is no longer fired from the cell, resulting in wave break up and potential v-fib. Alternans are seen on an organ-level scale in the ECG as microvolt T wave alternans (mTWA).

2.4 Electrical Restitution

Restitution of APD is where a change in APD is functionally related to a change in preceding DI as shown in Figure 2.3.

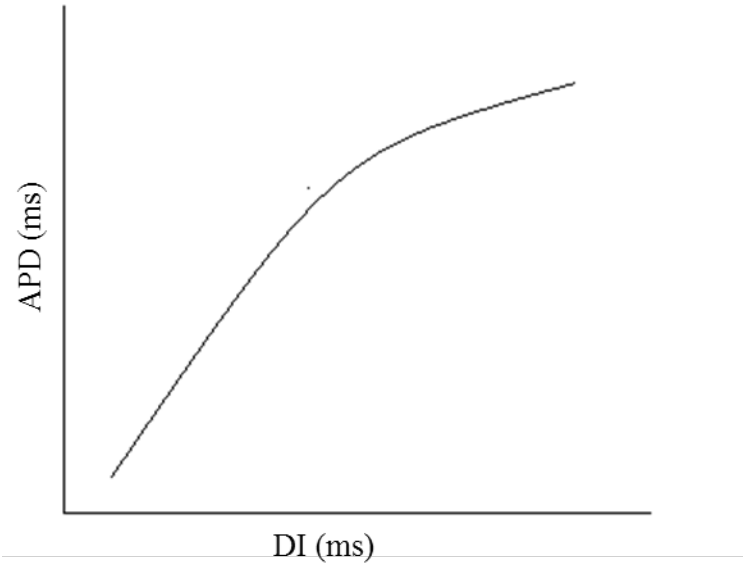

Figure 2.3 Schematic representation of the standard restitution curve. APD is shown as a function of DI. The curve has a higher slope at faster pacing rates and flattens out as DI increases.

If there is a sudden decrease in DI, i.e. a beat or stimulus comes earlier than expected, the resulting APD will be shortened and vice versa. In this way, the heart preserves time for the next DI, allowing the ventricles to fill with blood. Nolasco and Dahlen first described the importance of the slope, i.e. $\Delta APD/\Delta DI$, of the restitution function.[3] The slope has been used to predict occurrence of APD alternans with a slope of 1 defining the boundary of potential degeneration. The hypothesis states that a slope greater than 1 leads to unstable alternans while a slope less than 1 would create an environment free of alternans. A slope greater than 1 has been shown to lead to spiral wave break up.[5]

Flattening of the slope has been shown in pharmacological use and simulation to produce stabilizing, antiarrhythmic effects in some studies.[6, 7] This restitution function is thought to be one of the primary mechanisms of arrhythmia in addition to memory.

2.5 Cardiac Memory

Cardiac memory, where APD is dependent on several previous APs, also impacts electrical stability. First termed by Rosenbaum, cardiac memory is a characteristic seen in the T-wave of the ECG after induced pacing.[8] After pacing is completed, the T-wave continues to reflect the QRS complex (the beginning of contraction) vector from the previous pacing, until returning to normal after a certain period of time which is known as long-term memory. This phenomenon is also seen in APD, often referred to as short-term memory, where the effect only exists for seconds to minutes[9]—which is the type of cardiac memory this study focused on. Our lab has previously created protocols which explicitly control DI to allow for quantification of memory.[10] By stimulating the tissue in an oscillatory fashion, it is shown that two values of APD may exist at the same DI. The hysteresis that results from this method of pacing is used to quantify memory (See Methods for details). Memory has been shown to flatten the restitution curve, therefore it is hypothesized (or theorized) to make the tissue stable and move it away from a situation that would activate arrhythmia.[10-12] The effects of memory are argued to be as important as restitution in the mechanisms of arrhythmia.[13]

2.6 Heart Failure

Of Americans greater than 20 years of age, it is estimated that 5.1 million have HF.[14] HF may result from conditions including hypertension, myocardial infarction and various types of cardiomyopathy. The most common type of cardiomyopathy, dilated cardiomyopathy (DCM), results in weak, thin-walled ventricles. Ischemic cardiomyopathy (ICM) is caused by the loss of oxygen and glucose otherwise provided by normal blood flow to the tissue, and also results in weak, thin-walled ventricles. Hypertrophic cardiomyopathy (HCM) is the most common inherited heart condition and occurs in 1 in 500 individuals.[15] The thickening of the ventricular walls causes a loss in volume of the chambers—resulting in diastolic heart failure (DHF). Some populations

exhibit twice likely occurrence of SCD with a maximum wall thickness greater than 30mm.[16, 17]

Hypertrophic, ischemic and dilated hearts display altered gap junction distribution and density through the measurement of Cx43 in areas of structural damage, which contributes importantly to changes in conduction.[18-21] Studies have shown that an overwhelming majority of patients with ventricular arrhythmia also have structural heart disease (SHD).[22, 23] Ion currents such as I_{K1} and I_{Kr} have been shown to be downregulated in failing hearts resulting in delayed repolarization of the AP.[24] Changes in ion concentration, gap junctions, and structural integrity affect the propagation of conduction through the heart. The enhanced heterogeneity of these properties in failing hearts may lead to an association with higher occurrence of SCD.[25] These altered properties are manifestations of disease which may then induce additional deficiencies such as irregular electrical activity.

Chapter 3 METHODS AND ANALYSIS

3.1 Preparation of Samples and Experimental Setup

Tissues were excised from patients undergoing total heart replacement (THR) i.e. transplant or artificial heart implantation, or LVAD implantation. All procedures were approved by the University of Kentucky Institutional Review Board and subjects gave informed consent. Data were collected from 7 human hearts, 6 of which were failing. Of the failing hearts, 5 were from male patients with an average age of 49 years. Both RV and LV samples were obtained from two of the hearts (patients 2 and 3). Patient diagnoses consisted of DCM, ICM and idiopathic cardiomyopathy. For one tissue sample (patient 6), the only diagnosis that was available was DHF, but the tissue was noticeably hypertrophic. One LV tissue sample was available from a non-failing (NF) donor heart (M, 33 years). Patient and tissue details are shown in Table 3.1.

Table 3.1 Patient demographics and sample information. Sample type, procedure, diagnosis, age and sex are shown.

Patient	Samples	Procedure	Diagnosis	Age	Sex
1	LV	LVAD	DCM	32	F
2	LV, RV	THR	Idiopathic cardiomyopathy	21	M
3	LV, RV	THR	Idiopathic cardiomyopathy	52	M
4	LV	LVAD	ICM	51	M
5	LV	THR	ICM	64	M
6	RV	THR	DHF	72	M
NF	LV	THR	Non-Failing	33	M

After excision by the surgeon, the samples were preserved in ice cold saline solution in the operating room before transfer to an intermediate facility. The samples were placed in chilled Tyrode's solution for transport to the laboratory. Sample size varied from approximately 10x10x3 mm to 10x40x5 mm. Samples were pinned in a plastic chamber and superfused with Tyrode's solution bubbled with 95% O_2 and 5% CO_2, and maintained at 37±1˚C. The composition of the solution (for transport and superfusion) was (mmol/L): NaCl 137, KCl 4, $MgCl_2$ 0.5, NaH_2PO_4 1.8, $CaCl_2$ 2.7, glucose 5.5. The composition was modeled after Dangman et al[26] with a 25% increase in glucose in all

samples excluding tissue from patient 1. $NaHCO_3$ was added to the bubbled solution until a pH level of 7.35 ± 0.05 was reached. Tissues were stimulated with platinum-iridium bi-polar electrodes with a 3 ms pulse, amplitude of which was three to four times diastolic threshold at a basic constant CL of 850 ms. Tissue from patient 1 was paced at 500 ms. Transmembrane potential (TMP) recordings were made from the endocardial surface of the tissues with a glass microelectrode filled with 3M KCl. The TMPs were simultaneously digitized by two systems. In one, a custom developed control program made in LabVIEW digitized the TMPs and analyzed them in real time to control DIs independent of APDs. Details of this real time control of DIs are provided elsewhere.[10] At the same time, a commercial data acquisition system was used to digitize TMPs at a rate of 50,000 samples/s for storage. All subsequent analyses were conducted on the TMPs recorded using the commercial data acquisition system. Figure 3.1 shows the process described above.

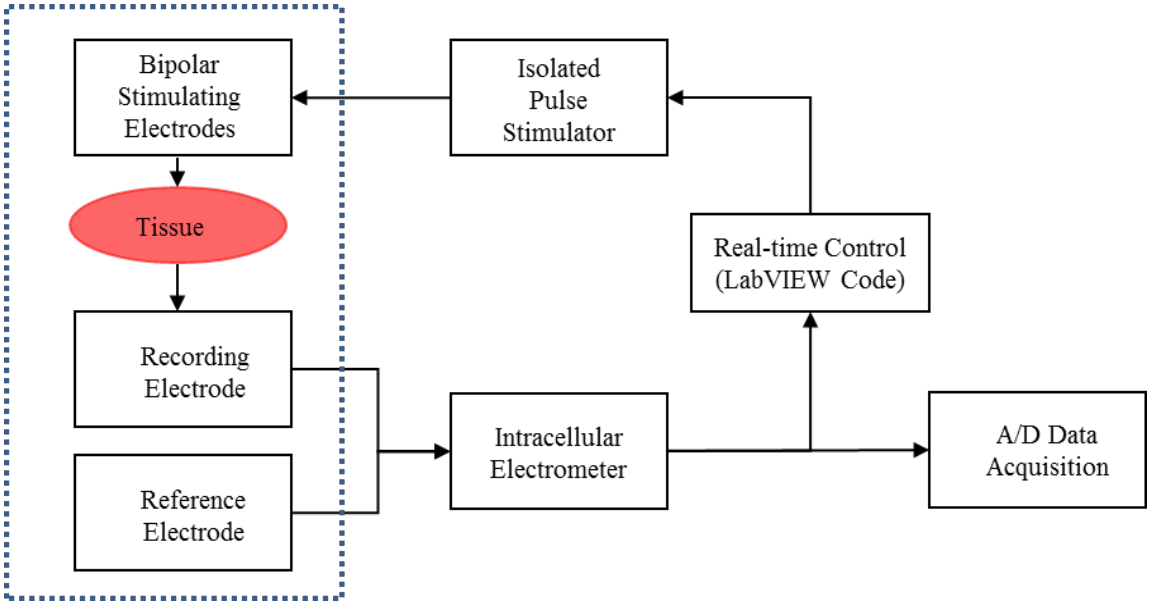

Figure 3.1 Process flow chart of experimental stimulation and recording. The process of stimulating and recording from the tissue is shown including the custom DI control. The dotted box represents the tissue chamber.

A custom program written in MATLAB (Mathworks, Natick MA, USA) was used to process the digitized TMPs offline. Before analyzing, data were digitally lowpass filtered with a cutoff frequency of 1000 Hz. The beginning of an AP was determined as the lowest point in the upstroke independent of the stimulus artifact. APD was calculated at either 90% or 70% repolarization. Although an automated program identified start and end of APs, all identifications were visualized and manually checked to confirm correct quantification of APDs.

3.2 Sinusoidal Protocols

In order to quantify memory in restitution of APD, two pacing protocols were used which consisted of twenty values of constant DI followed by two cycles of DIs oscillating in a sinusoidal pattern. The protocols, SIN 400 and SIN 150, consisted of a baseline DI of 400 (150) ms which oscillated between 100 (10) and 700 (290) ms and are illustrated in Figure 3.2.

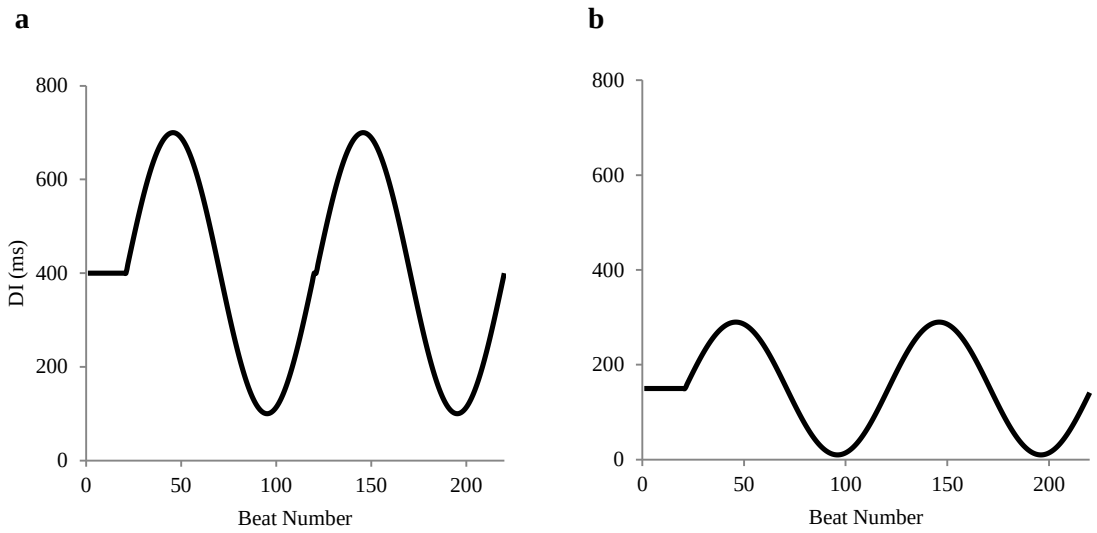

Figure 3.2 Sinusoidal protocols used to quantify memory. A baseline DI of 400ms (**a**) and 150ms (**b**) were used in protocols to quantify memory.

If there was drift in the APDs due to adaptation, a trend line fit between the two minima in the APD curves was subtracted from the APDs. Parameters of the hysteresis were measured from the second cycle of the protocols and included loop thickness, area, tilt,

maximum delay and minimum delay. The second cycle was used to allow for adequate adaptation of the tissues to take place. Loop thickness was measured as the difference in APDs at the center value of the DI. Loop area was calculated by using the MATLAB function polyarea. Loop tilt was calculated as the slope of a line fitted between the points of maximum and minimum DIs and their corresponding APDs. Maximum and minimum delays were calculated by first fitting a 2nd degree polynomial to the center 21 points surrounding a peak or a nadir in APDs and DIs. The delay was computed as the interval, in beats, between the maximum (or minimum) DI and maximum (or minimum) APD. An example of DIs and APDs resulting during a SIN 400 protocol, resulting hysteresis loop in restitution, and measured characteristics are shown in Figure 3.3.

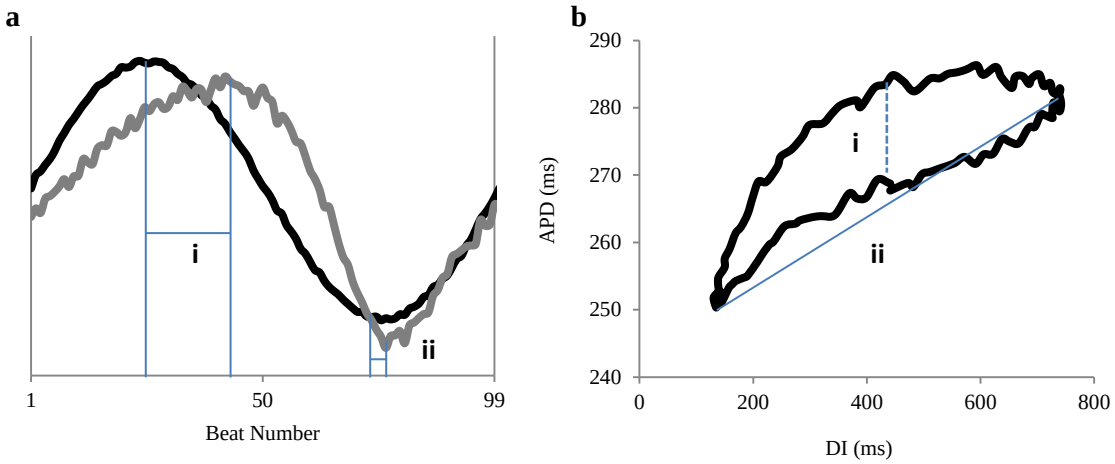

Figure 3.3 Example of SIN400 protocol and resulting hysteresis loop. (**a**) APD (gray) and DI (black) values from LV tissue from patient 1 with parameters of maximum delay (i) and minimum delay (ii). (**b**) This pacing results in a hysteresis loop with parameters of loop thickness (i), tilt (ii) and the area enclosed by the loop.

Average values for the group were calculated by first averaging all of the computed measures from multiple trials within a tissue and then across all tissue samples.

3.3 Standard and Dynamic Protocols

In order to obtain the standard restitution curve, the protocol consisted of a basic CL s1=500 ms with n=10 beats, and the s1-s2 interval was decremented in steps of 20 ms from 500 to 300 ms, steps of 10 ms from 300 ms until block (when the cell is unable to

fire an AP) occurred, as previously used by Narayan et al.[27] To obtain the dynamic restitution curve, stepwise pacing started at a CL of 800 ms with n=50 in each step. Steps were defined in decrements of 100 ms (for 800 ms to 500 ms), 50 ms (500 ms to 400 ms), 20 ms (400 ms to 300 ms) and 10 ms (300 ms until block occurred), as previously used by Runze and Patwardhan.[10] The standard and dynamic pacing protocols are shown in Figure 3.4.

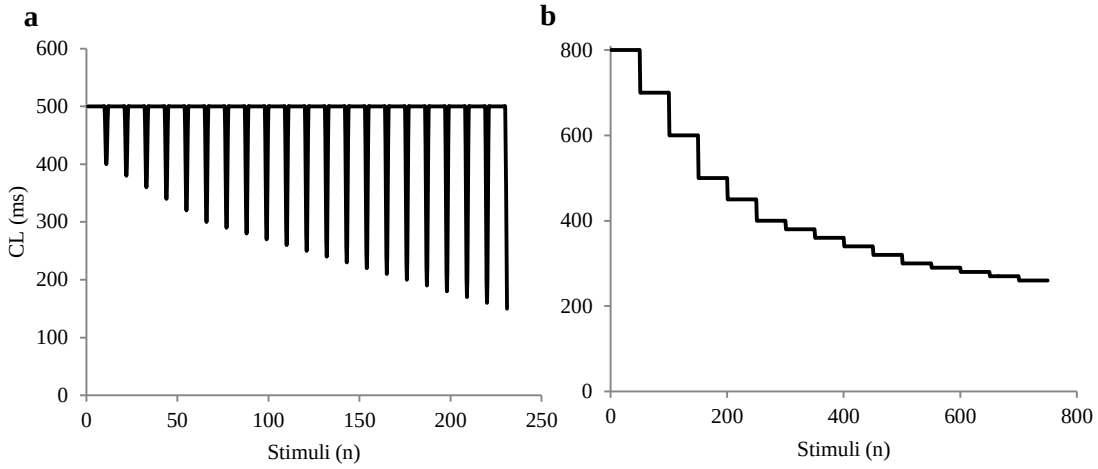

Figure 3.4 Standard and dynamic protocols. (**a**) Standard protocol with an s1 of 500 ms and decrementing steps of s1-s2 interval. (**b**) Dynamic stepwise protocol beginning at 800 ms until block.

All trials from each tissue were averaged to form an average restitution curve representative of that tissue. Slope of the restitution curve was determined by averaging the slopes between each pair of points within the range of DIs which contained all tissue samples.

3.4 Measurement of APD Alternans and dV/dt

Tissue from patient 2 and the non-failing data were not used in APD or dV/dt alternans analysis due to noise contamination. Because this analysis determines changes that occur on a beat by beat basis, we considered that the effect of noise on quantification of alternans of APD and dV/dt would be unacceptable and thus data from this tissue were not used in this analysis. Small fluctuations in data for restitution and hysteresis analysis were not as detrimental, because those measurements were taken from data across

multiple beats in which the resulting change in APD was greater than the contribution of noise. We investigated incidence of alternans of APD for those trials where the CL ≤500 ms. This limit was chosen based on a similar range that is used when detecting mTWA during stress tests, which is the contemporary clinical method of assessing risk of ventricular arrhythmia. Alternans was considered to occur when a beat by beat change in APD of ≥4 ms (same threshold as that used previously by Pruvot et al[28]), occurred on at least 5 successive beats. Incidence of occurrence of alternans was calculated as the percentage of pairs of alternating beats out of total pairs of beats. A 10-point smooth differentiation and low pass filter, "smooth_diff.m", was used on un-filtered TMPs to calculate the rate of depolarization in MATLAB. The maximum rate of depolarization, i.e. dV/dt_{max}, was quantified as the maximal dV/dt in the upstroke of the AP. As with quantification of APDs, all located dV/dt_{max} points were manually verified by the use to ensure independence of stimulus artifacts. Alternans of dV/dt_{max} was considered when there was an alternating magnitude change in dV/dt_{max} for successive beats (i.e. an increase-decrease-increase or decrease-increase-decrease). Alternans of dV/dt_{max} was considered in (out of) phase with APD alternans when the larger (smaller) dV/dt_{max} preceded the longer of the long-short APD sequence.[29] In calculations of incidences of alternans, because some trials had more APs than others, no more than 575 APs (the average number of APs from all trials) from any one trial were included in the percentages in order to avoid trials with substantially more APs weighing the percentage of incidence.

3.5 Computational Modeling

While we did receive one NF tissue for the study, lack of control, i.e. non-diseased heart tissues, is a limitation of our study. In order to obtain data to serve as surrogate for control tissues, simulations were performed using the O'Hara Rudy dynamic (ORd) model developed and made available by the Rudy Laboratory.[30] The ORd simulates human ventricular myocytes from endocardium, mid-myocardium and epicardium—the endocardium option was selected to match the experimental data. The code was modified to control the CL and DI as in the tissue experiments. Initial conditions were obtained by pacing the model at a constant CL of 850 ms until a steady state was reached to replicate

experimental conditions. Standard and dynamic restitution protocols were simulated for comparison with experimental data. Sinusoidal protocols were run in the simulation but the experimentally observed hysteresis was not replicated by the model (See Limitations).

3.6 Statistical Analysis

A one-sample, two-tailed t Test was used to compare the single values of restitution slopes and APD from simulation and NF with the multiple values from failing LV, i.e. assuming either the NF or simulation value was representative of the population mean (NF tissue). The n values from failing LV were tested against either NF or simulation to determine if there was a significant difference, meaning that the failing LV were from a different population than either NF tissue or simulation. A p value less than 0.05 was used to determine significance. The primary objective in our study was demonstration of phenomenon, i.e. the study was primarily of a discovery type. However, as a supplement to the analysis, statistical testing was performed when possible.

Chapter 4 RESULTS

4.1 AP Characteristics

An example of the TMPs recorded at basic pacing CL of 850 ms is shown in Figure 4.1. Average APDs at pacing CL of 850 ms for LV (n=4), RV (n=2), NF LV and simulation were 359.5, 339.4, 244.2 and 247.5 ms, respectively. Failing tissues showed prolonged APDs in comparison to the APDs from NF and from simulations, although the differences were not statistically significant (a consequence of large variation in the APDs in failing hearts and small sample size). The height of APs, i.e. AP amplitudes (APAs), was similar among all tissue samples, i.e. we did not see any systematic differences in APAs.

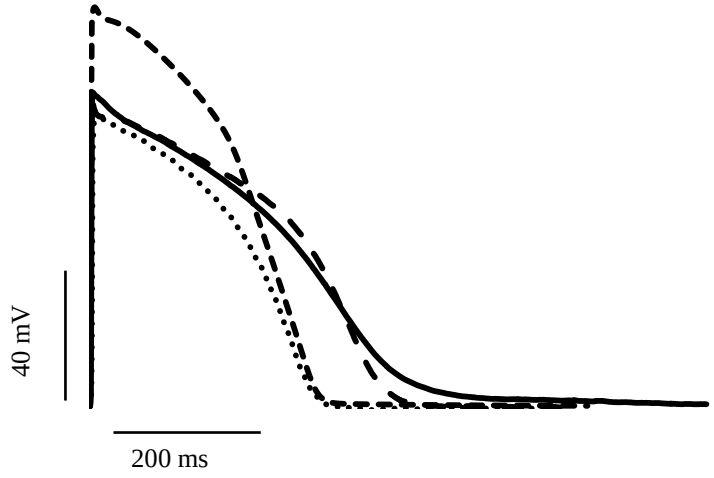

Figure 4.1 Representative single APs from tissues and simulation. NF LV (dotted), simulation (small dashed), failing RV (large dashed) and failing LV (solid) are shown at 850 ms CL.

4.2 Cardiac Memory

Hysteresis in restitution was observed in both failing and NF tissues. Successful protocols, i.e. those without spontaneous beats, and with a 1:1 response from stimulus to activation, were run in the failing LV for SIN 400 (n=5), SIN 150 (n=3), and in the failing RV for SIN 400 (n=3), and SIN 150 (n=1). Both SIN 400 and SIN 150 protocols

were successful in the NF LV tissue. As stated before, hysteresis in restitution could not be replicated in the simulation.

Of the calculated parameters of hysteresis, the largest differences between failing and NF LV tissues were seen in loop thickness, tilt and area in SIN400 protocols. Failing LV had a loop thickness of 17.6 ± 1.3 compared to the 8.05 ms thickness in NF tissue. Average loop tilt, an indicator of the slope of restitution, was 0.13 in failing LV vs 0.05 in NF LV. Area was also larger, 8745.6 in failing compared to 3709.1 ms^2 in NF. The differences between maximum and minimum delays were not statistically significant. Parameters of hysteresis computed during the SIN 400 protocols for all tissues are given in Table 4.1.

Table 4.1 Average hysteresis parameters of SIN400.. Thickness, tilt, area, maximum delay and minimum delay are shown in NF LV (n=1), LV (n=5) and RV (n=3) tissues with mean ± SEM. †Data were only available from one tissue sample with replicates. *$p<0.05$

Parameter	Non-Failing†	LV	RV
Thickness (ms)	8.05	17.6 ± 1.3*	22.6 ± 1.4
Tilt	0.05	0.13 ± 0.018*	0.14 ± 0.015
Area (ms^2)	3709.1	8745.6 ± 939.2*	10649 ± 1298
Max Delay (beats)	12.5	10.3 ± 1.5	8.7 ± 2.5
Min Delay (beats)	3	3 ± 0.4	3.2 ± 0.17

Examples of hysteresis loops from the LV during the SIN 400 protocol are shown in Figure 4.2. The results in Figure 4.2(a) illustrate the variation in hysteresis characteristics and baseline APDs that existed among diseased tissues. The differences between failing and NF LV in thickness, area and tilt are seen in Figure 4.2(b).

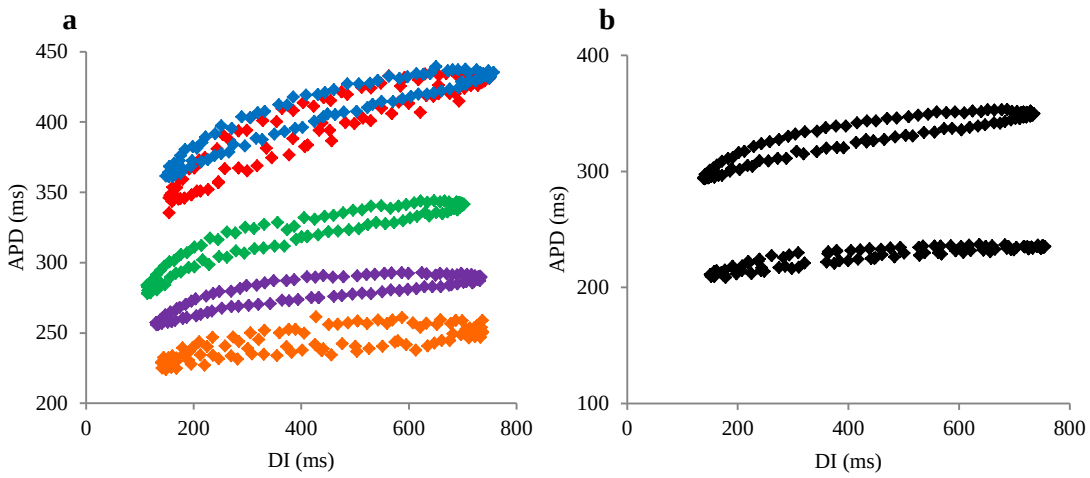

Figure 4.2 SIN400 LV hysteresis loops. (**a**) Average loops from SIN400 in failing LV tissues are shown. Tissues top to bottom are from patients 3 (blue), 2 (red), 5 (green), 1 (purple), 4 (orange). (**b**) Average loops from SIN400 failing LV (top) and non-failing LV (bottom) tissues are shown.

There was a significant difference between NF (1 beat) and failing (2.5 beats) LV tissue in the measurement of minimum delay during SIN150 protocols. No statistically significant differences were seen in the other characteristics of the SIN150 protocols (see Table 4.2).

Table 4.2 Average hysteresis parameters of SIN150. Thickness, tilt, area, maximum delay and minimum delay are shown in NF LV (n=1), LV (n=5), and RV (n=1) tissues with mean ± SEM. †Data were only available from one tissue sample with replicates. ‡Data were only available from one tissue sample and one trial. *p<0.05

Parameter	Non-Failing ‡	LV	RV †
Thickness (ms)	13.3	14.3 ± 1.5	17.2
Tilt	0.23	0.28 ± 0.057	0.25
Area (ms^2)	2357	2851.7 ± 285.8	3311.8
Max Delay (beats)	7	5.2 ± 0.73	5.5
Min Delay (beats)	1	2.5 ± 0.29*	2.5

Average loops from failing and non-failing LV during SIN150 are shown in Figure 4.3. In the NF tissue, the actual DI was slightly larger than the targeted DI due to conduction

delay, therefore shifting the protocol closer to DI 200, resulting in an increase of area and thickness and a decrease of tilt. This change counteracted any statistically significant differences which may have existed between the NF and failing LV tissues in the SIN150 protocols.

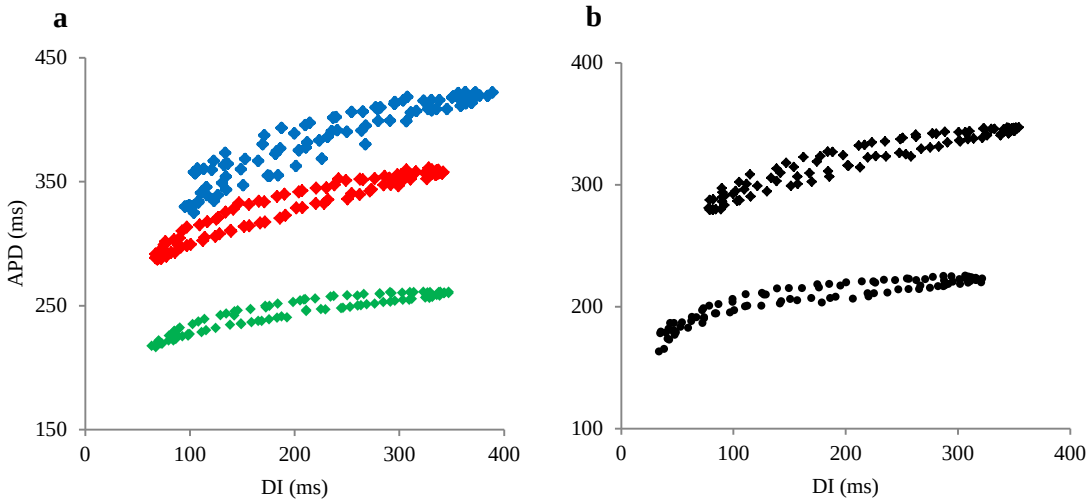

Figure 4.3 SIN150 LV hysteresis loops. (**a**) Average loops from SIN150 in failing LV tissues are shown. Tissues top to bottom are from patient 2 (blue), 3 (red), and 1 (green). (**b**) Average loops from SIN150 in failing (top) and non-failing (bottom) tissues are shown.

Thickness and area were higher in the RV compared to the LV, while tilt, maximum and minimum delays were mixed in both protocols. Loops characteristics within RV tissues were more similar than characteristics within LV tissues. The RV loops from SIN400 and SIN150 protocols are shown in Figure 4.4. Tissues 2 and 3, which both had diagnoses of idiopathic heart failure, had more similar loops in both the RV and LV as shown in Figures 4.2-4.

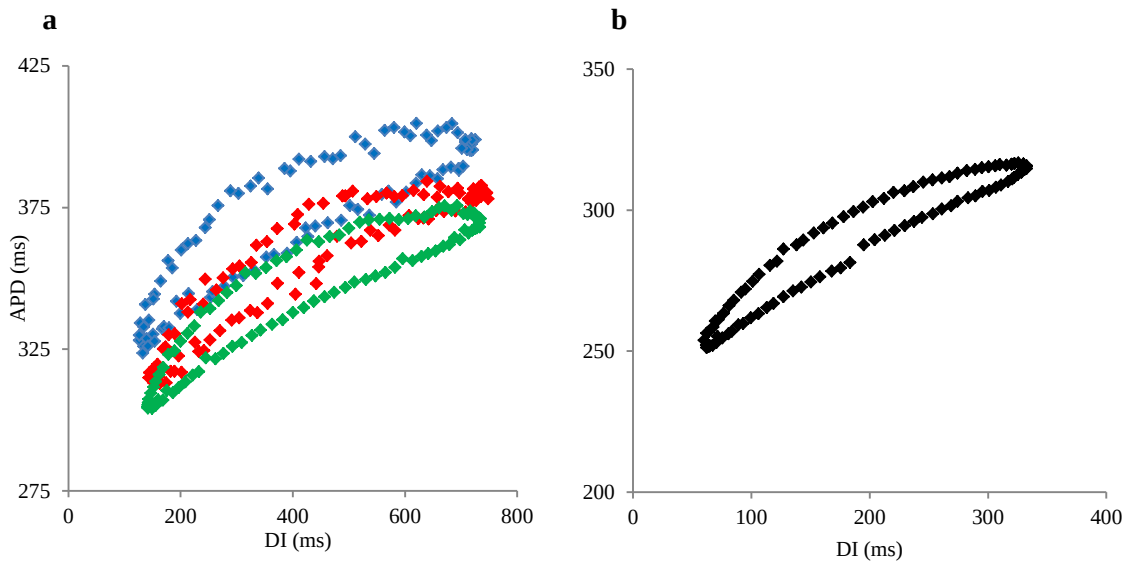

Figure 4.4 SIN400 and SIN150 RV hysteresis loops. (**a**) Average loops from SIN400 in failing RV tissues are shown. Tissues from top to bottom are from patients 2 (blue), 3 (single trial, red), and 6 (green). (**b**) Average loop from SIN150 in failing RV tissue from patient 6 is shown.

4.3 Electrical Restitution

Standard restitution curves were obtained in failing LV tissues (n=2), RV (n=2), NF LV, and in simulation. Dynamic restitution curves were obtained in LV (n=2), RV (n=3), NF LV, and in simulation. Slopes were calculated within the DI range where data were present from all tissue samples, which was DIs from 106 to 199 ms for the standard restitution and 210 to 484 ms for the dynamic restitution. Averaged slopes of restitution are shown in Table 4.3.

Table 4.3 Standard and dynamic restitution slopes. RV, LV, NF LV tissues and simulation slopes are shown as mean ± SEM. Slopes were obtained from the DI range which included all tissues.

Tissue	Standard	n	Dynamic	n
RV	0.62 ± 0.2	2	0.25 ± 0.1	3
LV	0.81 ± 0.4	2	0.48 ± 0.3	2
NF	0.14	1	0.16	1
SIM	0.14	1	0.09	1

Slopes from simulation and NF LV were lower than those from failing LV in standard and dynamic restitution protocols. Figure 4.5 illustrates the average curves from simulation, NF and failing LV tissues.

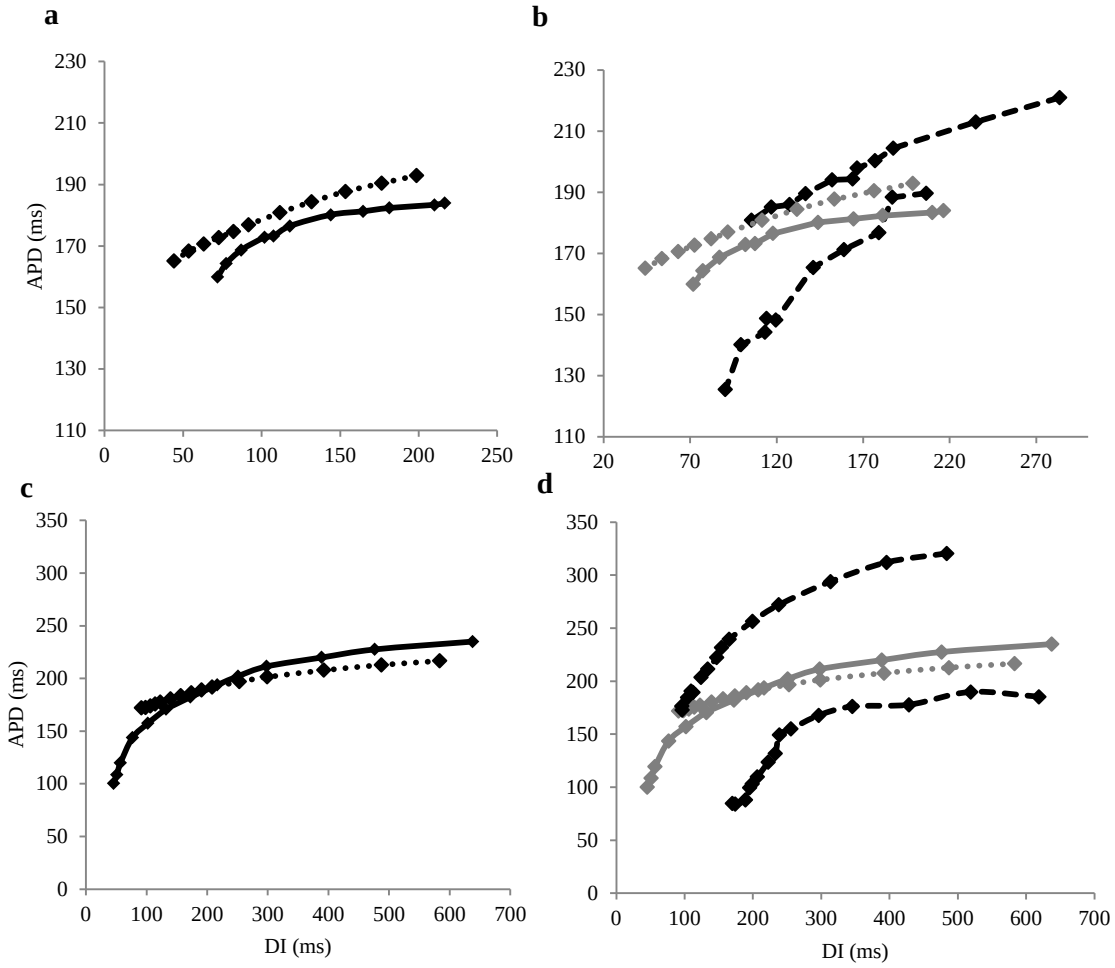

Figure 4.5 Standard and dynamic restitution curves in LV. (**a**) Standard restitution curves obtained from simulation (dotted) and non-failing LV tissue (solid). (**b**) Curves obtained from failing tissues from patient 5 (top) and patient 4 (bottom) are overlaid with the NF and simulation curves. (**c**) Dynamic restitution curves obtained from simulation (dotted) and non-failing LV tissue (solid). (**d**) Failing tissues from patient 3 (top) and patient 4 (bottom) are overlaid with the NF and simulation curves.

Slopes from RV in both standard and dynamic protocols were lower than failing LV but higher than simulation and NF LV. Figure 4.6 shows standard and dynamic restitution curves from the RV.

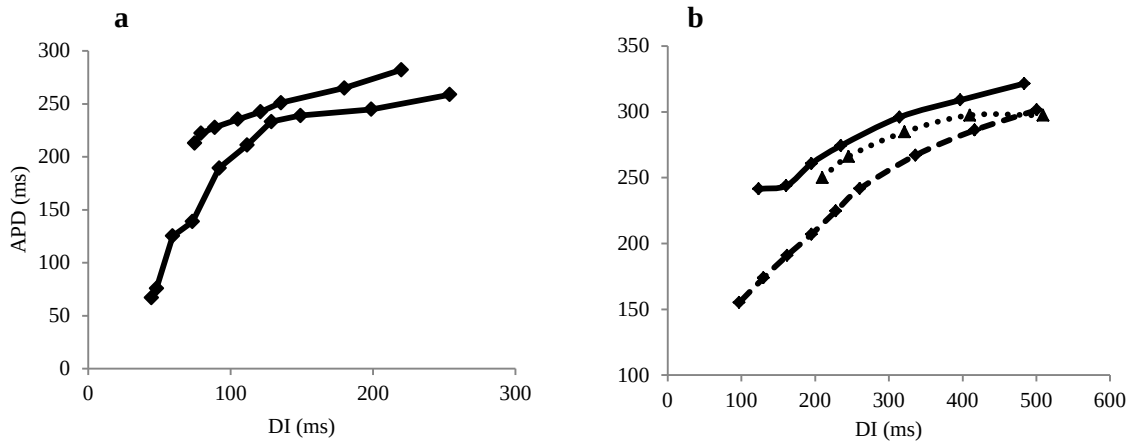

Figure 4.6 Standard and dynamic restitution curves in RV. (**a**) Standard restitution curves from failing RV patients 6 (top) and 3 (bottom). (**b**) Dynamic restitution curves from failing RV patients 3 (solid), 2 (dotted), and 6 (dashed).

4.4 APD Alternans and dV/dt Phase Behavior

TMPs recorded at all CLs 500 ms or shorter (i.e. faster activation rates) were analyzed for occurrence of alternans. As previously mentioned, trials from patient 2 (RV and LV), as well as the NF tissue, were not used due to noise. The total percentage of occurrence of alternans in LV (n=4) was 52% and RV (n=2) was 21%. Within this subset, i.e. when alternans of APD occurred, the percentage of in and out of phase relationship with dV/dt_{max} alternans was determined. Table 4.4 shows percentage of APs which had alternating behavior in each tissue and the phase relationship with dV/dt_{max} alternans.

Table 4.4 APD alternans, dV/dt_{max} and phase behavior. Occurrence of APD alternans, incidence of in-phase behavior, and the percent change in dV/dt_{max} during alternans are shown for tissues with data from CL≤500 ms. Data from patient 2 and NF LV tissue were not used due to noise.

Tissue	Patient	APs (n)	Alternating APs (n)	APD Alternans (%)	In Phase (%)	dV/dt_{max} (%)
LV	1	4092	2635	64.4	97.6	77
	3	3364	529	15.7	99.7	2.5
	4	2164	1909	88.3	85.5	3.8
	5	551	252	45.7	59.1	2.2
RV	3	1699	1546	91.0	100	149.6
	6	5783	0	0	--	--

Out of phase behavior was seen in all LV samples but the incidence varied; around 40% of APD alternans were out of phase with dV/dt_{max} alternans in patient 5, while other tissues showed less than 15% out of phase. The percent change in dV/dt_{max} during alternans of dV/dt_{max} ranged from very small to exceeding 105% in LV and 340% in RV in individual CL recordings. Figure 4.7 depicts the in phase and out of phase behavior seen in a single recording in tissue from patient 4.

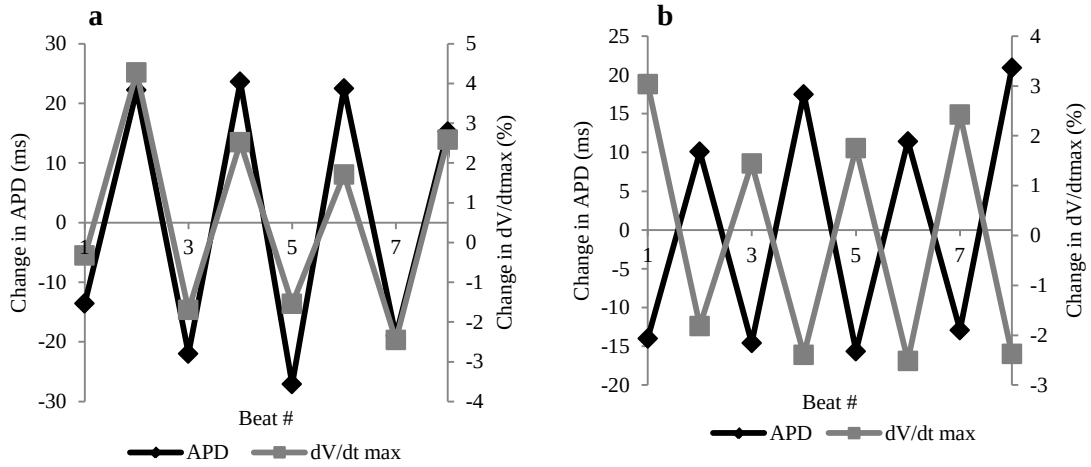

Figure 4.7 Example of in and out of phase behavior. (**a**) LV tissue from patient 4 was paced at CL 290 ms and exhibited in phase behavior between alternans of APD and dV/dt_{max} and (**b**) also exhibited out of phase behavior within the same trial.

Chapter 5 DISCUSSION

5.1 AP Characteristics

Although we were unable to obtain control data from RV tissues, consistent with our results from the LV, Lou et al showed a significant increase in APD in failing RV tissue, caused by downregulation of I_{K1} and I_{Kr}.[31] Beuckelmann showed a prolonged APD in patients with HF as well as a reduced I_{K1} and Ito_1.[32] These K^+ currents have a strong effect on phase 1 repolarization and the plateau shown in failing isolated cells.[33] Such decreases in K^+ currents can lead to early after depolarizations and arrhythmia. Longer APDs seen in failing tissues suggest these alterations exist and that these mechanically failing hearts provide favorable conditions for arrhythmia. Similar to the results reported by Glukhov et al, the tendency for prolongation of APD in failing LV, although not statistically significant, was also seen in our study.[34]

5.2 Cardiac Memory

Hysteresis in restitution of APD has been previously shown to exist in canine and swine tissues, two common animal models used during investigation of electrical stability.[10, 35] In this study, precisely controlled oscillatory changes in DI were used to demonstrate that in human ventricular tissues, restitution of APD also displays bifurcation and hysteresis similar to that seen in canines and swine. While there could be species differences, compared to healthy control tissues in swine reported by Jing et al, tilt was higher and maximum and minimum delays were smaller in the failing human tissue.[36] A higher tilt or equivalent for slope in this case, and lower measures of memory could be explained by the manifestation of disease in the human tissue. Calcium handling has been proposed to be a contributing variable of the existence of hysteresis.[11] Differences also exist in Ca^{2+}, such as reduced Ca^{2+} sequestration by the sarcoplasmic reticulum in diseased cells.[37] This reduction of Ca^{2+} in failing hearts could explain a decrease in memory. Our results of the sinusoidal protocol agree with the concept that there is a buildup of memory during increase in DI and a release of memory during a decrease in DI.[38, 39] Toal et al showed in humans, using monophasic action potential (MAP) recordings in ischemic hearts that short term memory (APD_n and APD_{n-1}) was more strongly correlated than restitution

(APD_n and DI_{n-1}) to APD variation during ventricular fibrillation (VF).[40] While the measures of hysteresis were mixed, the study of memory in addition to restitution is important for understanding and predicting electrical stability.

5.3 Electrical Restitution

Koller et al showed using MAP recordings that slopes of standard and dynamic restitution were larger in those with SHD compared to those without, but the differences were not statistically significant, similar to the results from our study.[41] The failing curve more obviously diverges with a higher slope from the NF and simulation curves, which remain somewhat flattened at higher pacing rates, as shown in Figure 4.5-6. The higher slope is consistent with decreased stability in the tissue, therefore increased probability for the tissue to degenerate into arrhythmia according to the contemporary hypothesis. It should be noted the slopes from the standard curve are from protocols which started at a CL of 500 ms, an already fast pacing rate compared to the dynamic restitution curves which began at a CL of 800 ms. Slopes measured across a range of values which included all tissue samples showed that the slopes in LV were greater than those in RV. Yue et al found that the slopes of activation recovery intervals (the duration between the maximum negative slope of the QRS complex and the maximum positive slope of the T wave in a unipolar extracellular ECG) were significantly higher in the LV than RV, using non-contact mapping in hearts without SHD.[42] An increase in heterogeneity between the ventricles, as seen in our study through the average values of APD and restitution slopes, may contribute to instability in those patients with failing hearts.

5.4 APD Alternans & dV/dt Phase Behavior

There have been mixed results on rate of depolarization of healthy and diseased tissues. Studies have found dV/dt_{max} in healthy human endocardial tissue to be 234 ± 28 V/s measured through microelectrode recordings[43] and 231 ± 30 V/s using patch clamp techniques.[44] Another study reported an average dV/dt_{max} of 297 ± 19 V/s found in diseased human endocardial tissues, in addition to a significantly longer APD in infarcted areas compared to non-infarcted zones.[26] In our study, dV/dt_{max} values varied and were often comparable to those reported previously even though the tissues were from failing

and NF hearts. Average dV/dt_{max} of the NF tissue at a CL of 850 was measured to be 103.0 V/s while average failing tissue (n=4) values ranged from 111.8 to 273.3 V/s. An average dV/dt_{max} as high as 364.85 was seen in a single recording from failing tissue.

In terms of incidence of alternans, we observed that recordings made at a CL 500 ms and shorter had an average 53.5% incidence of APD alternans in LV (n=4) and 45.5% in RV (n=2). Although we were unable to examine alternans in NF tissue, Koller et al showed that APD alternans first appeared at slower pacing rates in those with SHD and the magnitude of APD alternans was also greater in the failing tissues.[41] This supports the correlation between failing hearts and increased risk of ventricular arrhythmia as mTWA measured in ECG commonly occur with those at greater risk for ventricular arrhythmia.[45] Chauhan shows that individuals with cardiomyopathy and mTWA had higher heterogeneity in electrical properties across the tissue than control subjects. They claimed that those with mTWA therefore possessed a substrate favorable for conduction block and reentrant ventricular arrhythmias due to a steep repolarization gradient.[46]

Jing et al previously reported the existence of a phenomenon in swine and canines where dV/dt_{max} of the short AP was larger than that of the long AP, i.e. out of phase behavior between APD and dV/dt_{max} alternans.[29] That study showed that out of phase behavior prevented the transition of concordant alternans to discord and thus increased electrical stability. Results from this study show not only that this out of phase behavior also occurs in failing human ventricles, but that this phase also does change spontaneously. While it is unclear whether the incidence of out of phase behavior in failing hearts is more or less than that in normal healthy hearts, these results do support further investigation about the relationship between the independent changes in depolarization and repolarization phases during alternans of APD.

5.5 Heterogeneity

Heterogeneity in the tissue which is often caused by remodeling from disease, results in a pro arrhythmic substrate that is more vulnerable to SCD.[47-49] Specifically in HCM, there is an increase of heterogeneity within conduction of the ventricle[50] and increased activation delay in fibrotic tissue[51]. Large transmural APD gradients are seen in areas

with lowered Cx43 expression. The lack of Cx43 between tissue layers leads to lowered communication pathways, slowing conduction and may contribute to a pro-arrhythmic substrate.[52] The tissues in the current study often had fatty deposits and/or fibrosis. Although diagnosis of the failing tissues varied, similar characteristics were exhibited such as prolonged APD and increased restitution slopes which align with other studies.

This study examined the electrophysiological properties in human ventricular tissue, specifically the differences in hearts from patients with and without heart failure. We have shown for the first time in failing and non-failing human ventricular cells, the hysteresis in restitution of APD for quantification of memory and existence of spontaneous phase change between alternans of APD and dV/dt_{max}. These observational studies have allowed insight into how the electrical properties are altered in diseased tissue. Further understanding of these electrophysiological characteristics will help to elucidate the mechanisms which influence arrhythmia in diseased hearts.

Chapter 6 LIMITATIONS

As the tissues used in these experiments were explanted during transplant or LVAD implant, there were limitations in quantity and quality of the samples. Such limitations include not having an equal sized NF sample set or uniform diagnoses across patients. Additional control data would be needed for comparison of APD and dV/dt_{max} alternans between healthy and failing tissues. Sinusoidal protocols were simulated for comparison with experimental data; however, the ORd model did not replicate the hysteresis as was observed experimentally. The patient from whom the NF tissue was obtained suffered from head trauma and also had a history of barbiturates; it is unknown whether the barbiturates were in the patient's system at the time of death. The structural integrity and activity of the donor heart was assumed to be normal as the subject was free of heart disease. We also note, again, that the statistical analyses were included only as supplementary information because of very limited sample sizes for control tissues.

APPENDIX A

Tissue from patient 1 of the human study showed a double component bump in the foot and upstroke of the AP, independent of the stimulus artifact. When looking through other recordings, this phenomenon was also seen in swine RV post-chromanol and mouse ventricular tissue (unpublished data). An additional bump (as seen in human and mice) was displayed higher in the upstroke of the AP, sometimes creating a notch in the peak of the AP. The shape of the bump increased in sharpness with faster pacing rates. The double component AP occurred in the presence of APD and dV/dt alternans and without them in our data. Figure 1 shows an example of the characteristic seen in dilated human LV endocardium at a pacing CL of 220ms. The phenomenon is more subtle when looking at a string of APs (Figure 1a) and is detailed in Figure 1b-c of the upstroke of the AP.

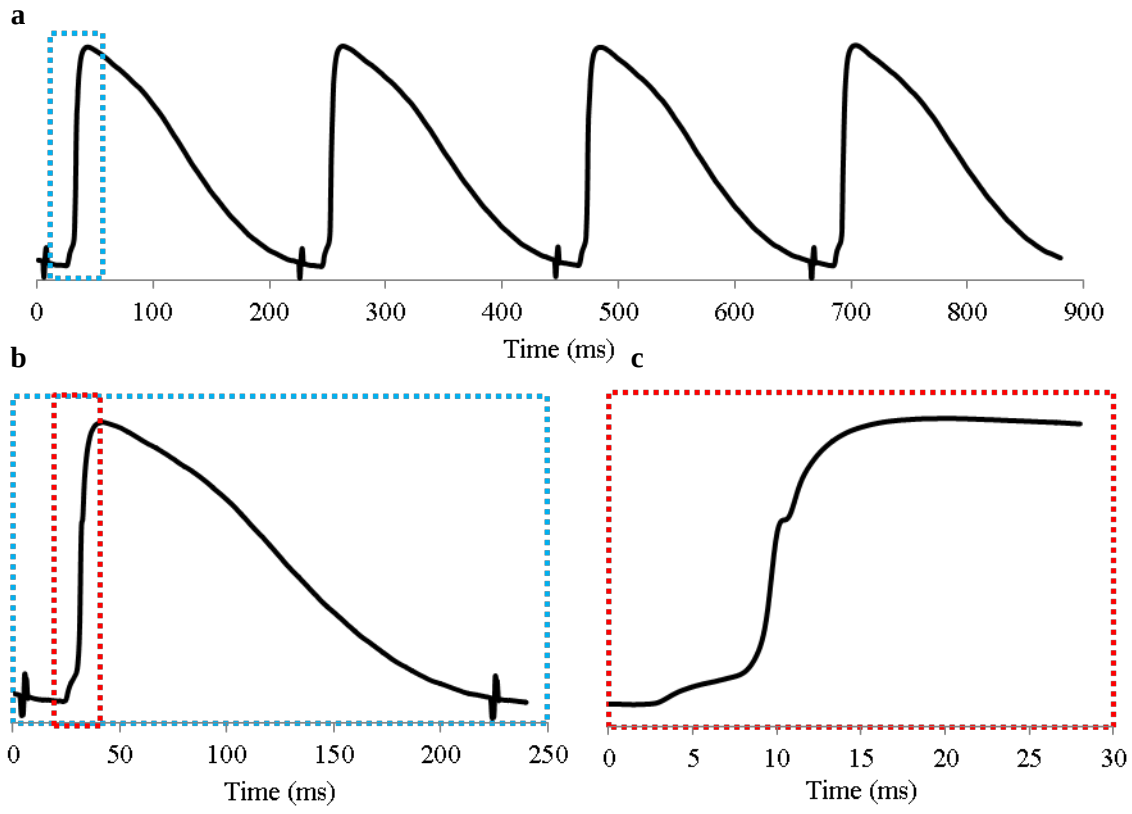

Figure 1. (**a**) APs from patient 1 with a pacing cycle length of 220ms. (**b**) A single AP shows the convex curve of the foot in the upstroke. (**c**) A second bump is seen higher in the upstroke of the AP while examining the depolarization of the AP.

As dV/dt_{max} decreased with increasing pacing rates, the dV/dt_{max} of the bump also decreased. The time between the two dV/dt_{max} values increased with pacing rate, showing the sharpness of the bump as seen in Figure 2 in the mouse.

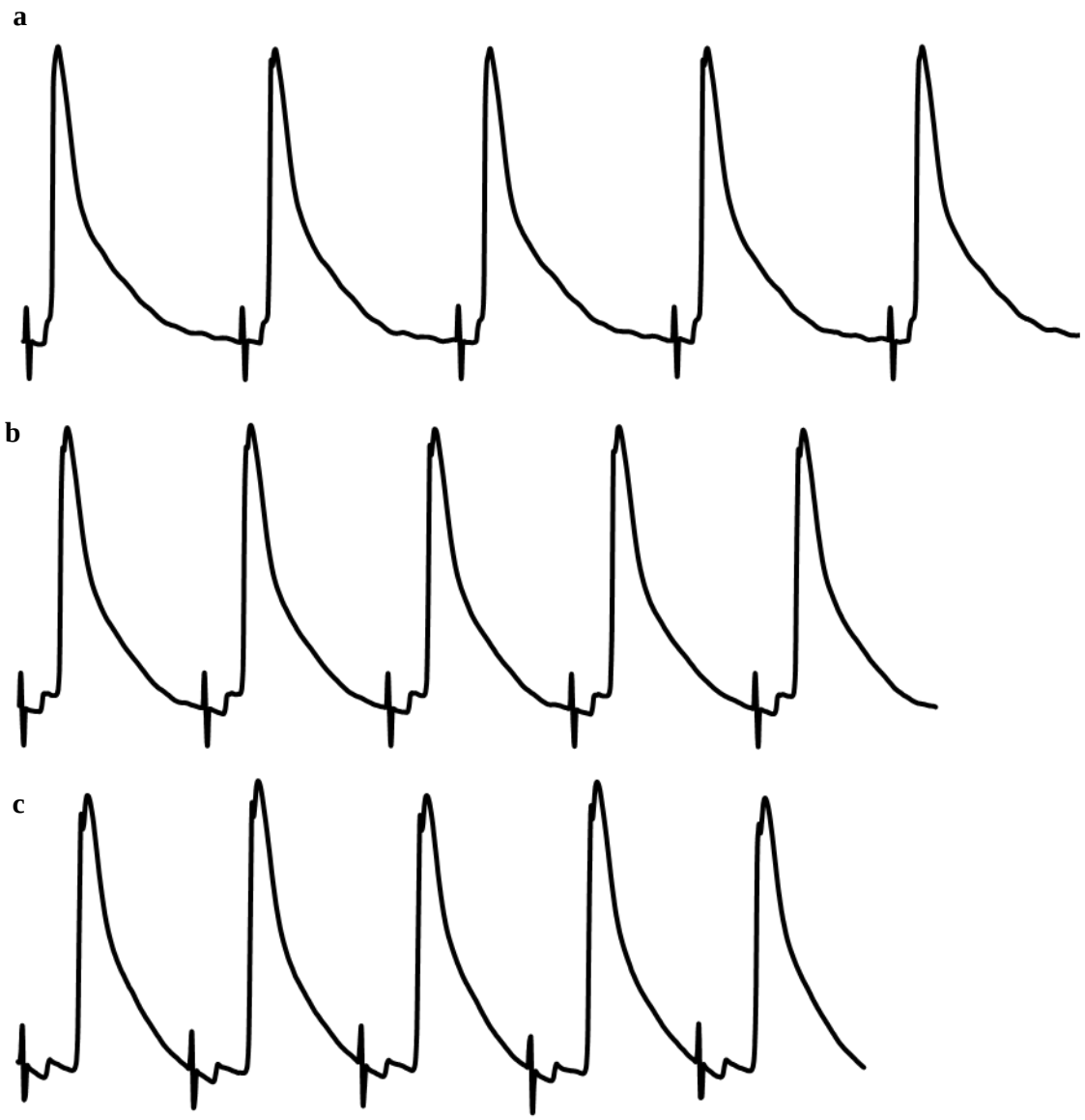

Figure 2. Traces of APs from mouse ventricle are shown at 140 (**a**), 120 (**b**) and 115ms (**c**) cycle length illustrating the morphology of the double component seen in the foot and upstroke. The second bump is seen interacting with the peak of the AP, creating a notch.

This accentuated foot in the AP has been shown to exist due to conduction across high resistance gaps *in silico*. Simulation of conduction across sucrose gaps resulted in a pronounced foot.[53] Vasquez and Moreno showed in simulation that conduction across fibroblasts through electrotonic interaction was possible—the same bump existed, coupled with a slower conduction velocity (CV) and lower dV/dt.[54] Longer electrotonic feet have been seen in the AP in addition to Wenckebach sequences when examining conduction across a sucrose gap.[55] Wenckebach sequence, known as Type1 AV heart block, is caused by increasing PR interval (the second portion of the diastolic interval) until the next beat is unable to be conducted, resulting in block. The cycle then repeats when the cell is able to fire again. This bump results in an increased conduction delay. The same pattern was shown to exist due to ischemia vs normal tissue and included slower upstrokes.[56] This double component has been seen in rabbit cells and shown to increase the latency period.[57] As shown previously in the mouse, the bump was much more noticeable and distinctly at the foot of the AP, almost isolated during very fast pacing rates. Hoshino also showed the response of the double component morphed as cycle length changed.[58] Double components of the AP may result from a mismatch, or difficulty transferring current across certain cells.[59, 60] Hoshino showed the existence of postrepolarization refractoriness and Wenckebach patterns in guinea pig ventricular myocytes due to the effects of I_{Ks} on the refractory period and I_{K1} on the shape of the foot potentials. Amin showed the decrease in I_{Na} in patients with Brugada syndrome, resulting in a sloped upstroke and decreased dV/dt. Sometimes a delayed after depolarization (DAD) masked under the following AP as a bump in the foot potential.[61]

Previous studies indicate that the double component behavior observed in tissues from our lab is probably due to electrotonic interactions of a changed substrate, whether a physical or chemical alteration. The phenomenon was observed over a wide range of cycle lengths recorded and was shown to exist across multiple species, diagnoses and drug treatments. While the mouse and swine tissues were assumed to be healthy, local differences in pathways may have contributed to the bumps observed. The mouse ventricles were not isolated from the rest of the organ, allowing for additional pathways and increased heterogeneity. Drug treatment with Chromanol, an I_{Ks} antagonist, was shown to prolong APD and increase restitution slope, thickness and area in swine right

ventricle.[36] This reduction in I_{Ks}, as previously mentioned, affects the refractory period which may result in abnormal behavior, e.g. Wenckebach sequence. The cause of the phenomenon observed in diseased human tissue could be attributed to more diverse factors such as ion currents and fibrosis. A higher resistance path could be explained in part due to the dilated nature of the tissue from patient 1. These interactions result in increased conduction delay, i.e. slower CV, which may lead to block. These examples found through observational discovery illustrate that ventricular tissues across multiple species may exhibit the same characterized “bump” phenomenon. Whether tissues which have multiple irregular properties (i.e. more vulnerable substrates) result in a higher likelihood of such bumps, and whether these bumps contribute to arrhythmic events is uncertain.

REFERENCES

1. McNally B, Robb R, Mehta M, Vellano K, Valderrama AL, Yoon PW, Sasson C, Crouch A, Perez AB, Merritt R, Kellermann A, Centers for Disease C, Prevention. Out-of-hospital cardiac arrest surveillance --- cardiac arrest registry to enhance survival (cares), united states, october 1, 2005--december 31, 2010. *Morbidity and mortality weekly report. Surveillance summaries*. 2011;60:1-19
2. Singh SN, Carson PE, Fisher SG. Nonsustained ventricular tachycardia in severe heart failure. *Circulation*. 1997;96:3794-5
3. Nolasco JB, Dahlen RW. A graphic method for the study of alternation in cardiac action potentials. *Journal of applied physiology*. 1968;25:191-6
4. Wu R, Patwardhan A. Mechanism of repolarization alternans has restitution of action potential duration dependent and independent components. *Journal of cardiovascular electrophysiology*. 2006;17:87-93
5. Fenton FH, Cherry EM, Hastings HM, Evans SJ. Multiple mechanisms of spiral wave breakup in a model of cardiac electrical activity. *Chaos*. 2002;12:852-92
6. Weiss JN, Garfinkel A, Karagueuzian HS, Qu Z, Chen PS. Chaos and the transition to ventricular fibrillation: A new approach to antiarrhythmic drug evaluation. *Circulation*. 1999;99:2819-26
7. Garfinkel A, Kim YH, Voroshilovsky O, Qu Z, Kil JR, Lee MH, Karagueuzian HS, Weiss JN, Chen PS. Preventing ventricular fibrillation by flattening cardiac restitution. *Proceedings of the National Academy of Sciences of the United States of America*. 2000;97:6061-66
8. Rosenbaum MB, Blanco HH, Elizari MV, Lazzari JO, Davidenko JM. Electrotonic modulation of the t wave and cardiac memory. *The American journal of cardiology*. 1982;50:213-22
9. Gilmour RF, Jr., Otani NF, Watanabe MA. Memory and complex dynamics in cardiac purkinje fibers. *The American journal of physiology*. 1997;272:H1826-32
10. Wu R, Patwardhan A. Restitution of action potential duration during sequential changes in diastolic intervals shows multimodal behavior. *Circulation research*. 2004;94:634-41
11. Guzman KM, Jing L, Patwardhan A. Effects of changes in the l-type calcium current on hysteresis in restitution of action potential duration. *Pacing and clinical electrophysiology : PACE*. 2010;33:451-9
12. Chialvo DR, Michaels DC, Jalife J. Supernormal excitability as a mechanism of chaotic dynamics of activation in cardiac purkinje fibers. *Circulation research*. 1990;66:525-45
13. Cherry EM, Fenton FH. Suppression of alternans and conduction blocks despite steep apd restitution: Electrotonic, memory, and conduction velocity restitution effects. *American journal of physiology. Heart and circulatory physiology*. 2004;286:H2332-41
14. Go AS, Mozaffarian D, Roger VL, Benjamin EJ, Berry JD, Blaha MJ, Dai S, Ford ES, Fox CS, Franco S, Fullerton HJ, Gillespie C, Hailpern SM, Heit JA, Howard VJ, Huffman MD, Judd SE, Kissela BM, Kittner SJ, Lackland DT, Lichtman JH, Lisabeth LD, Mackey RH, Magid DJ, Marcus GM, Marelli A, Matchar DB, McGuire DK, Mohler ER, 3rd, Moy CS, Mussolino ME, Neumar RW, Nichol G,

Pandey DK, Paynter NP, Reeves MJ, Sorlie PD, Stein J, Towfighi A, Turan TN, Virani SS, Wong ND, Woo D, Turner MB, American Heart Association Statistics C, Stroke Statistics S. Heart disease and stroke statistics--2014 update: A report from the american heart association. *Circulation*. 2014;129:e28-e292

15. Maron BJ, McKenna WJ, Danielson GK, Kappenberger LJ, Kuhn HJ, Seidman CE, Shah PM, Spencer WH, 3rd, Spirito P, Ten Cate FJ, Wigle ED, Task Force on Clinical Expert Consensus Documents. American College of C, Committee for Practice Guidelines. European Society of C. American college of cardiology/european society of cardiology clinical expert consensus document on hypertrophic cardiomyopathy. A report of the american college of cardiology foundation task force on clinical expert consensus documents and the european society of cardiology committee for practice guidelines. *Journal of the American College of Cardiology*. 2003;42:1687-713
16. Spirito P, Bellone P, Harris KM, Bernabo P, Bruzzi P, Maron BJ. Magnitude of left ventricular hypertrophy and risk of sudden death in hypertrophic cardiomyopathy. *The New England journal of medicine*. 2000;342:1778-85
17. Elliott PM, Gimeno Blanes JR, Mahon NG, Poloniecki JD, McKenna WJ. Relation between severity of left-ventricular hypertrophy and prognosis in patients with hypertrophic cardiomyopathy. *Lancet*. 2001;357:420-4
18. Peters NS, Green CR, Poole-Wilson PA, Severs NJ. Reduced content of connexin43 gap junctions in ventricular myocardium from hypertrophied and ischemic human hearts. *Circulation*. 1993;88:864-75
19. Smith JH, Green CR, Peters NS, Rothery S, Severs NJ. Altered patterns of gap junction distribution in ischemic heart disease. An immunohistochemical study of human myocardium using laser scanning confocal microscopy. *The American journal of pathology*. 1991;139:801-21
20. Kostin S, Rieger M, Dammer S, Hein S, Richter M, Klovekorn WP, Bauer EP, Schaper J. Gap junction remodeling and altered connexin43 expression in the failing human heart. *Molecular and cellular biochemistry*. 2003;242:135-44
21. Wiegerinck RF, van Veen TA, Belterman CN, Schumacher CA, Noorman M, de Bakker JM, Coronel R. Transmural dispersion of refractoriness and conduction velocity is associated with heterogeneously reduced connexin43 in a rabbit model of heart failure. *Heart rhythm : the official journal of the Heart Rhythm Society*. 2008;5:1178-85
22. Sacher F, Tedrow UB, Field ME, Raymond JM, Koplan BA, Epstein LM, Stevenson WG. Ventricular tachycardia ablation: Evolution of patients and procedures over 8 years. *Circulation. Arrhythmia and electrophysiology*. 2008;1:153-61
23. Swerdlow CD, Winkle RA, Mason JW. Determinants of survival in patients with ventricular tachyarrhythmias. *The New England journal of medicine*. 1983;308:1436-42
24. Nabauer M, Kaab S. Potassium channel down-regulation in heart failure. *Cardiovascular research*. 1998;37:324-34
25. Tomaselli GF, Marban E. Electrophysiological remodeling in hypertrophy and heart failure. *Cardiovascular research*. 1999;42:270-83

26. Dangman KH, Danilo P, Jr., Hordof AJ, Mary-Rabine L, Reder RF, Rosen MR. Electrophysiologic characteristics of human ventricular and purkinje fibers. *Circulation*. 1982;65:362-8
27. Narayan SM, Franz MR, Lalani G, Kim J, Sastry A. T-wave alternans, restitution of human action potential duration, and outcome. *Journal of the American College of Cardiology*. 2007;50:2385-92
28. Pruvot EJ, Katra RP, Rosenbaum DS, Laurita KR. Role of calcium cycling versus restitution in the mechanism of repolarization alternans. *Circulation research*. 2004;94:1083-90
29. Jing L, Agarwal A, Chourasia S, Patwardhan A. Phase relationship between alternans of early and late phases of ventricular action potentials. *Frontiers in physiology*. 2012;3:190
30. O'Hara T, Virag L, Varro A, Rudy Y. Simulation of the undiseased human cardiac ventricular action potential: Model formulation and experimental validation. *PLoS computational biology*. 2011;7:e1002061
31. Lou Q, Janks DL, Holzem KM, Lang D, Onal B, Ambrosi CM, Fedorov VV, Wang IW, Efimov IR. Right ventricular arrhythmogenesis in failing human heart: The role of conduction and repolarization remodeling. *American journal of physiology. Heart and circulatory physiology*. 2012;303:H1426-34
32. Beuckelmann DJ, Nabauer M, Erdmann E. Alterations of k+ currents in isolated human ventricular myocytes from patients with terminal heart failure. *Circulation research*. 1993;73:379-85
33. Nabauer M, Beuckelmann DJ, Erdmann E. Characteristics of transient outward current in human ventricular myocytes from patients with terminal heart failure. *Circulation research*. 1993;73:386-94
34. Glukhov AV, Fedorov VV, Lou Q, Ravikumar VK, Kalish PW, Schuessler RB, Moazami N, Efimov IR. Transmural dispersion of repolarization in failing and nonfailing human ventricle. *Circulation research*. 2010;106:981-91
35. Jing L, Chourasia S, Patwardhan A. Heterogeneous memory in restitution of action potential duration in pig ventricles. *Journal of electrocardiology*. 2010;43:425-32
36. Jing L, Brownson K, Patwardhan A. Role of slow delayed rectifying potassium current in dynamics of repolarization and electriccal memory in swine ventricles. *Journal of physiological science*. 2014;64:185-193
37. Beuckelmann DJ, Nabauer M, Erdmann E. Intracellular calcium handling in isolated ventricular myocytes from patients with terminal heart failure. *Circulation*. 1992;85:1046-55
38. Koller ML, Riccio ML, Gilmour RF, Jr. Dynamic restitution of action potential duration during electrical alternans and ventricular fibrillation. *The American journal of physiology*. 1998;275:H1635-42
39. Fox JJ, McHarg JL, Gilmour RF, Jr. Ionic mechanism of electrical alternans. *American journal of physiology. Heart and circulatory physiology*. 2002;282:H516-30
40. Toal SC, Farid TA, Selvaraj R, Chauhan VS, Masse S, Ivanov J, Harris L, Downar E, Franz MR, Nanthakumar K. Short-term memory and restitution during

ventricular fibrillation in human hearts: An in vivo study. *Circulation. Arrhythmia and electrophysiology*. 2009;2:562-70
41. Koller ML, Maier SK, Gelzer AR, Bauer WR, Meesmann M, Gilmour RF, Jr. Altered dynamics of action potential restitution and alternans in humans with structural heart disease. *Circulation*. 2005;112:1542-8
42. Yue AM, Franz MR, Roberts PR, Morgan JM. Global endocardial electrical restitution in human right and left ventricles determined by noncontact mapping. *Journal of the American College of Cardiology*. 2005;46:1067-75
43. Drouin E, Charpentier F, Gauthier C, Laurent K, Le Marec H. Electrophysiologic characteristics of cells spanning the left ventricular wall of human heart: Evidence for presence of m cells. *Journal of the American College of Cardiology*. 1995;26:185-92
44. Pereon Y, Demolombe S, Baro I, Drouin E, Charpentier F, Escande D. Differential expression of kvlqt1 isoforms across the human ventricular wall. *American journal of physiology. Heart and circulatory physiology*. 2000;278:H1908-15
45. Rosenbaum DS, Jackson LE, Smith JM, Garan H, Ruskin JN, Cohen RJ. Electrical alternans and vulnerability to ventricular arrhythmias. *The New England journal of medicine*. 1994;330:235-41
46. Chauhan VS, Downar E, Nanthakumar K, Parker JD, Ross HJ, Chan W, Picton P. Increased ventricular repolarization heterogeneity in patients with ventricular arrhythmia vulnerability and cardiomyopathy: A human in vivo study. *American journal of physiology. Heart and circulatory physiology*. 2006;290:H79-86
47. Spear JF, Horowitz LN, Hodess AB, MacVaugh H, 3rd, Moore EN. Cellular electrophysiology of human myocardial infarction. 1. Abnormalities of cellular activation. *Circulation*. 1979;59:247-56
48. Nass RD, Aiba T, Tomaselli GF, Akar FG. Mechanisms of disease: Ion channel remodeling in the failing ventricle. *Nature clinical practice. Cardiovascular medicine*. 2008;5:196-207
49. Boukens BJ, Christoffels VM, Coronel R, Moorman AF. Developmental basis for electrophysiological heterogeneity in the ventricular and outflow tract myocardium as a substrate for life-threatening ventricular arrhythmias. *Circulation research*. 2009;104:19-31
50. Saumarez RC, Camm AJ, Panagos A, Gill JS, Stewart JT, de Belder MA, Simpson IA, McKenna WJ. Ventricular fibrillation in hypertrophic cardiomyopathy is associated with increased fractionation of paced right ventricular electrograms. *Circulation*. 1992;86:467-74
51. Kawara T, Derksen R, de Groot JR, Coronel R, Tasseron S, Linnenbank AC, Hauer RN, Kirkels H, Janse MJ, de Bakker JM. Activation delay after premature stimulation in chronically diseased human myocardium relates to the architecture of interstitial fibrosis. *Circulation*. 2001;104:3069-75
52. Poelzing S, Rosenbaum DS. Altered connexin43 expression produces arrhythmia substrate in heart failure. *American journal of physiology. Heart and circulatory physiology*. 2004;287:H1762-70
53. Janse MJ, van Capelle FJ. Electrotonic interactions across an inexcitable region as a cause of ectopic activity in acute regional myocardial ischemia. A study in intact

porcine and canine hearts and computer models. *Circulation research*. 1982;50:527-37
54. Vasquez C, Moreno AP, Berbari EJ. Modeling fibroblast-mediated conduction in the ventricle. *Comput. Cardiol.* 2004;31:349-52
55. Jalife J, Moe GK. Excitation, conduction, and reflection of impulses in isolated bovine and serum cardiac purkinje fibers. *Circulation research*. 1981;49:233-47
56. Lazzara R, El-Sherif N, Scherlag BJ. Disorders of cellular electrophysiology produced by ischemia of the canine his bundle. *Circulation research*. 1975;36:444-54
57. Yehia AR, Shrier A, Lo KC, Guevara MR. Transient outward current contributes to wenckebach-like rhythms in isolated rabbit ventricular cells. *The American journal of physiology*. 1997;273:H1-11
58. Hoshino K, Anumonwo J, Delmar M, Jalife J. Wenckebach periodicity in single atrioventricular nodal cells from the rabbit heart. *Circulation*. 1990;82:2201-16
59. de Bakker JM, Loh P, Hocini M, Thibault B, Janse MJ. Double component action potentials in the posterior approach to the atrioventricular node: Do they reflect activation delay in the slow pathway? *Journal of the American College of Cardiology*. 1999;34:570-7
60. Delmar M, Michaels DC, Jalife J. Slow recovery of excitability and the wenckebach phenomenon in the single guinea pig ventricular myocyte. *Circulation research*. 1989;65:761-74
61. Amin AS, Tan HL, Wilde AA. Cardiac ion channels in health and disease. *Heart rhythm : the official journal of the Heart Rhythm Society*. 2010;7:117-26

VITA

Author's Name: Kathleen Brownson

Birthplace: New Orleans, LA

Education: B.S. in Engineering Physics, Murray State University, Murray, KY 2011

Publications: Jing L, Brownson K, Patwardhan A. Role of slow delayed rectifying potassium current in dynamics of repolarization and electrical memory in swine ventricles. *Journal of physiological science.* 2014;64:185-193. DOI: 10.1007/s12576-014-0310-2